AIMS Materials Science, 5(1): 75–92.
DOI: 10.3934/matersci.2018.1.75
Received: 18 November 2017
Accepted: 17 January 2018
Published: 22 January 2018

http://www.aimspress.com/journal/Materials

Research article

Multi-response optimization of machining characteristics in ultrasonic machining of WC-Co composite through Taguchi method and grey-fuzzy logic

Ravi Pratap Singh[1], Ravinder Kataria[2,*], Jatinder Kumar[1] and Jagesvar Verma[2]

[1] Department of Mechanical Engineering, National Institute of Technology, Kurukshetra, Haryana, India
[2] School of Mechanical Engineering, lovely Professional University, Jalandhar, Punjab, India

*** Correspondence:** Email: kataria.ravinder07@gmail.com; ravinder.21852@lpu.co.in.

Abstract: This article addresses the application of grey based fuzzy logic coupled with Taguchi's approach for optimization of multi performance characteristics in ultrasonic machining of WC-Co composite material. The Taguchi's L-36 array has been employed to conduct the experimentation and also to observe the influence of different process variables (power rating, cobalt content, tool geometry, thickness of work piece, tool material, abrasive grit size) on machining characteristics. Grey relational fuzzy grade has been computed by converting the multiple responses, i.e., material removal rate and tool wear rate obtained from Taguchi's approach into a single performance characteristic using grey based fuzzy logic. In addition, analysis of variance (ANOVA) has also been attempted in a view to identify the significant parameters. Results revealed grit size and power rating as leading parameters for optimization of multi performance characteristics. From the microstructure analysis, the mode of material deformation has been observed and the critical parameters (i.e., work material properties, grit size, and power rating) for the deformation mode have been established.

Keywords: composite; grey-fuzzy; machining; optimization; Taguchi; USM; WC-Co

Abbreviations: GRFG: Grey relation fuzzy grade; OA: Orthogonal array; *MF*: Membership function; GRC: Grey relation coefficient; *R*: No. of replications; MRR: Material removal rate; *P*: Probability value; DOF: Degrees of freedom; TWR: Tool wear rate; *F*: Fisher's ratio; S/N: Signal-to-noise ratio

1. Introduction

Ultrasonic machining (USM) is a contemporary manufacturing method usually employed for processing materials with higher hardness/brittleness such as quartz, semiconductor materials, ceramics etc. [1]. Ultrasonic machining is also termed as ultrasonic drilling, ultrasonic abrasive machining, ultrasonic grinding, ultrasonic cutting, ultrasonic dimension machining, and slurry drilling. In USM, tool vibrates along its longitudinal axis at high frequency; usually greater than 20 kHz with amplitude of 12–50 μm. Abrasive slurry, which is a mixture of abrasive material such as silicon carbide, boron carbide and alumina suspended in water or some suitable carrier medium, is continuously pumped across the gap between the tool and work. The vibration of the tool causes the abrasive particles held in the slurry to impact the work surface, leading to material removal by micro-chipping.

Power rating and abrasive grit size are the main significant factors which affect the material removal rate (MRR) and tool wear rate (TWR) [2]. Lalchhuanvela et al. [3] presented a study of the MRR and surface roughness in machining of ceramics (alumina based). It was reported that the higher level of the input parameters gives higher MRR. Surface roughness (SR) was reported to be decreased with the reduction in grit size and power rating. Slurry concentration, flow rate of slurry and feed rate of tool have less effect on surface roughness. Komaraiah and Reddy [4], Kumar and Khamba [5], and Dam et al. [6] assessed the impact of work material properties on machining characteristics in ultrasonic machining. Results reported that work materials with higher fracture toughness and hardness tend to be machined at higher removal rates. Kataria et al. [7] reported that power rating and grit size are the most significant parameters that affect the hole quality in ultrasonic machining. Table 1 shows a summary of few studies reported on ultrasonic machining.

Tungsten carbide-cobalt (WC-Co) composite is classed among the most important metal matrix composite materials manufactured by a process called as “powder metallurgy” [8]. Several steps are included in the production of WC-Co composite, such as making of tungsten carbide powder, consolidation of the powder, sintering in the liquid phase and post-sintering operations. WC-Co composite materials are also known as cemented carbide, hard metal and in some cases, cermets [8]. WC-Co composite materials possess excellent hardness with toughness, wear resistance, good dimensional stability and high mechanical strength. Owing to their superior properties, these materials cover a wide range of industrial applications, e.g., manufacturing of wear parts, cutting and drilling tools, die and punch manufacturing.

Many investigators have studied the machinability of WC-Co composite materials using conventional and non-conventional techniques other than USM [8–15]. However, these techniques have their own limitations, in the perspective of deteriorated surface quality (cracks, heat affected zone, recast layer), high cutting forces and alteration of mechanical properties. These defects result into decrease in hardness, wear resistance and corrosion resistance of the machined components and also affect the product quality.

Ultrasonic machining could be a potential solution for addressing the problems related to machinability of WC-Co material. The process generally does not cause any significance alteration in the properties by means of surface damage [7]. Therefore, an attempt has been made to further explore the machining efficiency in ultrasonic drilling of WC-Co composites. So, this current article is targeted to optimize the process parameters (cobalt content, work material thickness, profile of tool, tool material, abrasive grit size, and power rating) in the ultrasonic machining of WC-Co

composites using grey-fuzzy logic. Figure 1 presents a graphic representation of the various inputs and output characteristics considered for the study.

Table 1. A summary of few studies reported on ultrasonic machining.

S. No	Investigator	Work material	Process variables	Results/Findings
1.	Ramulu M [16]	Silicon carbide, Titanium diborid/ Silicon carbide (TiB_2/SiC)	Abrasive material, Grit size	Over cut and taper increased with an increase in grit size for SiC work material. TiB_2/SiC has good machining characteristics as compare to SiC as work material in USM.
2.	Kumar V, Khamba JS [17]	Stellite 6 (Cobalt alloy)	Tool material, Abrasive, Slurry concentration, Grit size, Power rating	Optimized Setting: Titanium (ASTM Gr. 2); Abrasive: Al_2O_3; Slurry concentration: 25%; Grit size: 500; Power: 125 W (25%)
3.	Kumar J, Khamba JS, Mohapatra SK [18]	Pure Titanium (ASTM Grade-I)	Tool material, Abrasive, Grit size, Power rating, Slurry concentration	Tool material and power rating affects the rate of wear of the tool very significantly. Slurry concentration is insignificant parameter. Optimized Setting: titanium alloy, alumina, 500, 100 W, 30%.
4.	Hocheng H, Kuo KL, Lin JT [19]	Zirconia (Ceramic)	Static load, Amplitude	An increase in static load caused into decreased tool wear and hole clearance. Larger amplitude results in larger tool wear. Better surface roughness can be obtained when the amplitude is set at the mid-range.
5.	Singh R, Khamba JS [20]	Titanium (ASTM Gr. 2) and Titanium (ASTM Gr. 5)	Work material, Tool material, Abrasive, Power rating	An increase in MRR found with power rating. But sometimes MRR also decreased because of strain hardening of work piece. The best results have been obtained with SS tool and boron carbide slurry.
6.	Majeed MA, Vijayaraghvan L, Malhotra SK, et al. [21]	Al_2O_3/$LaPO_4$ composite	Work material, Tool (Solid and hollow)	Higher the hardness of the material, better the machining performance. Hollow tool gives more MRR as compare to solid tool. AE clearly indicate good machinability with 70:30 composite.
7.	Kumar J, Khamba JS, Mohapatra SK [22]	Pure Titanium (ASTM grade-I)	Tool material, Grit size, Power rating	For MRR and TWR, all the parameters were found to be significant and for SR only grit size was significant. Optimized Result For MRR: HCS, 220, 400 W. Optimized Result For TWR: titanium alloy, 500, 200 W. Optimized Result For SR: both tool material, 500, 300 W.
8.	Dvivedi A, Kumar P [23]	Titanium (ASTM Gr. 2) and Titanium (ASTM Gr. 5)	Work material, Grit size, Slurry concentration, Power rating, Tool material	Surface roughness was more for ASTM Grade 2 as compare to ASTM Grade 5. The percentage contributions of significant parameters as: grit size (33.90%), slurry concentration (40.38%), and tool (4.57%). Optimized Setting: ASTM Gr. 2, 320, 25%, 40%, HSS.
9.	Komaraiah M, Manan MA, Reddy PN, et al. [24]	Glass, Ferrite Porcelain, Alumina and Carbides.	Work material, Tool material	The material which have higher H/E ratio tends to have higher out-of-roundness. The rotary USM is more superior to conventional USM.
10.	Kumar J, Khamba JS [25]	Pure Titanium (ASTM grade-I)	Tool material, Abrasive, Grit size, Power rating	For TWR, tool material is the most significant parameter. For SR, grit size is the most significant parameter. Optimized Setting: Titanium alloy (ASTM Gr. 5), alumina, 500, 100 W (20%) for both response).

ASTM: American Society for Testing and Materials; SS: stainless steel; SR: surface roughness; HCS: High carbon steel.

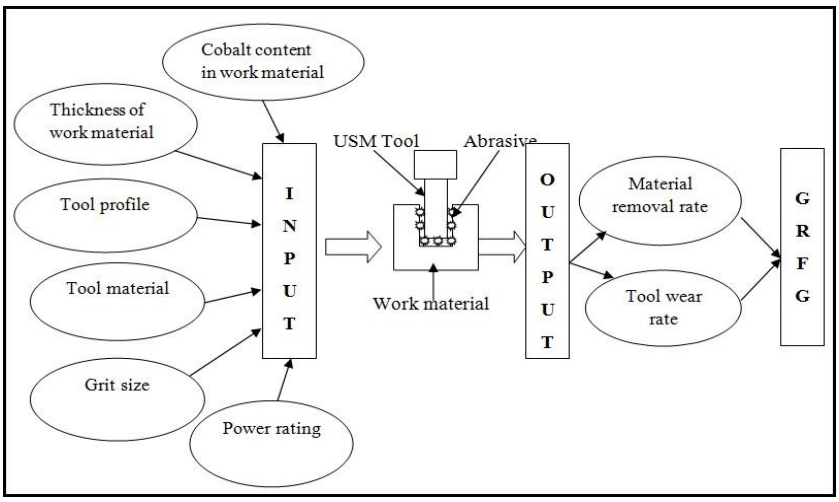

Figure 1. Process variables and responses of interest.

2. Materials and methods

In this article, work materials with the cobalt content of 6 wt% (hardness-1580 HV_{30}) and 24 wt% (hardness-780 HV_{30}), with 3 mm and 5 mm thickness were selected. The mechanical properties are shown in Table 2. The materials used for fabricating are the tools, stainless steel, silver steel and nimonic-80A respectively. Tools were designed to have same mass (9 g), the value of which was derived to obtain the resonant frequency. Two profiles of tool namely, hollow and solid have been fabricated. Boron carbide was used as abrasive, with three levels for mean particle size (mesh 200, 320 and 500). The concentration (by weight) of the abrasive slurry was decided to be fixed at 25%. Power rating was selected at three discrete levels as 40%, 60% and 80%. Table 3 shows the details of input parameters considered for the investigation.

Table 2. WC-Co composite materials and their characteristics.

		WC-6%Co	WC-24%Co
Chemical composition	WC	94%	76%
	Co	6%	24%
Mechanical properties	Density (g/cm^2)	14.9	12.9
	Hardness, H (HV_{30})	1580	780
	Elastic modulus, E (GPa)	630	470
	Fracture toughness (MPa·m$^{1/2}$)	9.6	14.5
	H/E ratio	2.5	1.65
	Thermal conductivity (W/mK)	80	50
	Coefficient of thermal expansion ($\times 10^{-6}$/K)	5.5	7.5

The experiments were performed on an "AP-450 model" (Sonic-Mill, Albuquerque, USA) ultrasonic machine set-up. The different components of USM setup are abrasive slurry supply system, transducer, coupler, horn, dial assembly, locking knob, converter and coupler clamp. Machining zone containing workpiece, fixture, and tool is depicted in Figure 2. MRR was computed by dividing the loss of weight (after machining) with the machining duration for drilling to the required depth. The stop watch was used to record the time taken for each experiment. The weight

was measured with an electronic balance (CIL, model-CA124), with least count of 0.0001 g. In the same way, tool wear rate was computed.

Table 3. Input parameters considered for the investigation.

Symbol	Parameter	Level 1	Level 2	Level 3
A	Cobalt content	6%	24%	
B	Thickness of work	3 mm	5 mm	
C	Profile of tool	Solid	Hollow	
D	Tool material	Stainless steel	Silver steel	Nimonic-80A
E	Grit size (mesh no.)	200	320	500
F	Power rating	40% (180 W)	60% (270 W)	80% (360 W)
Constant parameter				
Frequency of vibration	20 kHz	Slurry concentration	25%	
Static load	1.63 kg	Slurry temperature	25 ℃	
Amplitude of vibration	25.3–25.8 μm	Slurry flow rate	50×10^3 mm^3/min	

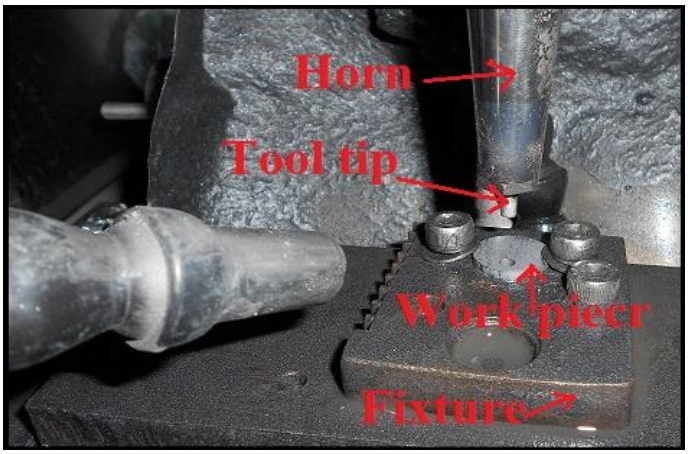

Figure 2. Machining zone.

3. Experimentation and data collection

This study makes use of Taguchi's L-36 OA for design of the experimental plan. There are three factors with two levels and remaining factors have three levels. In addition, three interactions (A × D, B × D, C × D) are also required to be evaluated. Therefore, the degrees of freedom of L-36 array (35 DOF) are adequately enough for the problem under consideration (with required DOF being 15). The experimental plan is exhibited in Table 4. Two replicates were run for the full experiment, and all of the trials were completely randomized to entertain the nuisance factors. Following relations are utilized for assessment of the S/N ratio [26].

Larger the best

$$\left(S/N\right)_{\mathrm{LB}} = -10\log\left(\frac{1}{R}\sum_{j=1}^{R}\frac{1}{y_j^2}\right) \tag{1}$$

Smaller the best

$$\left(S/N\right)_{SB} = -10\log\left(\frac{1}{R}\sum_{j=1}^{R} y_j^2\right) \quad (2)$$

where y_j is the response value recorded in j^{th} observation. Here, for MRR, "larger the best" and for TWR, "smaller the best" type S/N ratio were computed. Minitab-16 software has been utilized for analyzing the results.

Table 4. Experimental plan and results.

Exp No.	Parameters						MRR		TWR	
	A	B	C	D	E	F	Mean	S/N ratio	Mean	S/N ratio
1	1	1	1	1	1	1	0.0112	−39.04	0.0041	47.72
2	1	1	1	1	2	2	0.0126	−38.03	0.0030	50.23
3	1	1	1	1	3	3	0.0124	−38.42	0.0029	50.67
4	1	2	2	1	1	1	0.0058	−45.42	0.0029	50.88
5	1	2	2	1	2	2	0.0163	−35.87	0.0040	47.96
6	1	2	2	1	3	3	0.0138	−37.32	0.0038	48.45
7	2	1	2	1	1	1	0.0071	−44.10	0.0023	52.90
8	2	1	2	1	2	2	0.0170	−35.92	0.0046	46.81
9	2	1	2	1	3	3	0.0140	−37.14	0.0033	49.58
10	2	2	1	1	1	1	0.0055	−45.43	0.0022	53.18
11	2	2	1	1	2	2	0.0071	−43.03	0.0019	54.22
12	2	2	1	1	3	3	0.0071	−43.48	0.0016	55.70
13	1	1	1	2	1	2	0.0171	−35.38	0.0037	48.50
14	1	1	1	2	2	3	0.0248	−32.28	0.0050	45.97
15	1	1	1	2	3	1	0.0032	−51.15	0.0018	55.13
16	1	2	2	2	1	2	0.0210	−33.59	0.0041	47.81
17	1	2	2	2	2	3	0.0404	−27.89	0.0062	44.15
18	1	2	2	2	3	1	0.0046	−46.78	0.0019	54.39
19	2	1	2	2	1	2	0.0199	−34.01	0.0045	47.00
20	2	1	2	2	2	3	0.0295	−30.60	0.0055	45.24
21	2	1	2	2	3	1	0.0031	−50.82	0.0014	56.73
22	2	2	1	2	1	2	0.0093	−40.81	0.0028	51.10
23	2	2	1	2	2	3	0.0132	−37.57	0.0027	51.34
24	2	2	1	2	3	1	0.0027	−52.28	0.0013	57.86
25	1	1	1	3	1	3	0.0423	−27.58	0.0107	39.37
26	1	1	1	3	2	1	0.0111	−39.27	0.0026	51.67
27	1	1	1	3	3	2	0.0056	−45.09	0.0021	53.48
28	1	2	2	3	1	3	0.0396	−28.12	0.0073	42.73
29	1	2	2	3	2	1	0.0070	−43.31	0.0019	54.44
30	1	2	2	3	3	2	0.0173	−35.26	0.0046	46.75
31	2	1	2	3	1	3	0.0436	−27.28	0.0111	39.10
32	2	1	2	3	2	1	0.0113	−39.36	0.0024	52.54
33	2	1	2	3	3	2	0.0070	−43.31	0.0022	53.30
34	2	2	1	3	1	3	0.0275	−31.24	0.0083	41.54
35	2	2	1	3	2	1	0.0067	−43.53	0.0025	52.04
36	2	2	1	3	3	2	0.0040	−48.05	0.0015	56.68

4. Multi-response optimization using grey-fuzzy logic approach

In ultrasonic machining, the MRR and TWR are highly correlated responses. High MRR and low TWR cannot be achieved simultaneously for a particular control setting. For industrial applications, it is essential to obtain those machining solutions that could optimize the multiple responses concurrently. In this regard, grey fuzzy logic is employed for multi-response optimization.

4.1. GRA method

Grey relation analysis (GRA) is an effective method used for solving the complicated interrelationship among the data when the trends of their development are either homogeneous or heterogeneous. The major advantages of GRA method are real data based results, computations are simpler and easier to apply. For the problems related to manufacturing technology, the best decisions can be made by employing this method [27,28].

In this approach, the experimental data (MRR and TWR) is scaled and normalized, to fit in a range (0 to 1). The relationship between required (or desired) and actual (or experimental data) is expressed by computing grey relational coefficient through normalized data. The MRR is considered as "higher the best", while the TWR is considered as "lower the best" type response. The scaled values for both the responses are obtained using Eqs 3 and 4. Table 5 shows the normalized value for MRR and TWR.

The MRR ("higher the best" response) has been scaled as follows:

$$Z_{jys} = \frac{Z_{jyi} - \min Z_{yi}}{\max Z_{yi} - \min Z_{yi}} \tag{3}$$

While TWR ("lower the best" response) has been scaled as follows:

$$Z_{jys} = \frac{\max Z_{yi} - Z_{yi}}{\max Z_{yi} - \min Z_{yi}} \tag{4}$$

where, $\min Z_{yi} = \min\{Z_{1yi}, Z_{2yi}, \ldots\ldots, Z_{myi}\}$ and $\max Z_{yi} = \max\{Z_{1yi}, Z_{2yi}, \ldots\ldots, Z_{myi}\}$.

The GRC (γ_{jy}) for y^{th} response in j^{th} trial can be computed as:

$$\gamma_{jy} = \frac{\Delta_y^{min} + \xi \Delta_y^{max}}{\Delta_{jy} + \xi \Delta_y^{max}} \tag{5}$$

where, $\Delta_{jy} = |1 - Z_{jys}|$, $\Delta_y^{min} = \min\{\Delta_{1y}, \Delta_{2y}, ..., \Delta_{my}\}$, $\Delta_y^{max} = \max\{\Delta_{1y}, \Delta_{2y}, ..., \Delta_{my}\}$ and ξ is expressed as distinguishing coefficient ($\xi \in [0,1]$), and usually its value is set as 0.5. It is used for modification (expansion/contraction) of the range of grey relation coefficient.

Table 5. Results of grey relation analysis and fuzzy grade.

Exp. No.	Normalized value		Grey relation coefficient		GRFG
	MRR	TWR	MRR	TWR	
1	0.208	0.715	0.706	0.411	0.782
2	0.242	0.823	0.674	0.378	0.850
3	0.237	0.834	0.678	0.375	0.850
4	0.076	0.842	0.868	0.373	0.553
5	0.333	0.725	0.601	0.408	0.820
6	0.271	0.747	0.648	0.401	0.847
7	0.108	0.902	0.823	0.357	0.607
8	0.350	0.667	0.588	0.428	0.766
9	0.276	0.795	0.644	0.386	0.850
10	0.068	0.909	0.880	0.355	0.540
11	0.108	0.934	0.823	0.349	0.605
12	0.108	0.968	0.823	0.341	0.602
13	0.352	0.751	0.587	0.400	0.853
14	0.540	0.624	0.481	0.445	0.873
15	0.012	0.954	0.976	0.344	0.500
16	0.447	0.718	0.528	0.411	0.916
17	0.922	0.500	0.352	0.500	0.850
18	0.046	0.939	0.915	0.347	0.500
19	0.421	0.677	0.543	0.425	0.885
20	0.655	0.574	0.433	0.465	0.861
21	0.010	0.985	0.981	0.337	0.500
22	0.161	0.848	0.756	0.371	0.650
23	0.257	0.860	0.661	0.368	0.850
24	0.000	1.000	1.000	0.333	0.500
25	0.968	0.036	0.341	0.933	0.350
26	0.205	0.867	0.709	0.366	0.812
27	0.071	0.917	0.876	0.353	0.546
28	0.902	0.388	0.357	0.563	0.796
29	0.105	0.940	0.826	0.347	0.600
30	0.357	0.664	0.583	0.430	0.760
31	1.000	0.000	0.333	1.000	0.500
32	0.210	0.893	0.704	0.359	0.833
33	0.105	0.912	0.826	0.354	0.602
34	0.606	0.281	0.452	0.640	0.650
35	0.098	0.879	0.836	0.363	0.592
36	0.032	0.983	0.940	0.337	0.500

4.2. Fuzzy logic optimization

An imprecision based mathematical approach used to form an intensive relationship across the inputs and outputs is termed as “fuzzy logic”. Fuzzy system encompasses of basic components such as fuzzy sets, fuzzy inference, fuzzy rules, membership functions and defuzzification. The mapping is formulated from the input to output through fuzzy logic, by the process of fuzzy inference. The fuzzy logic mechanism has been detailed in Figure 3.

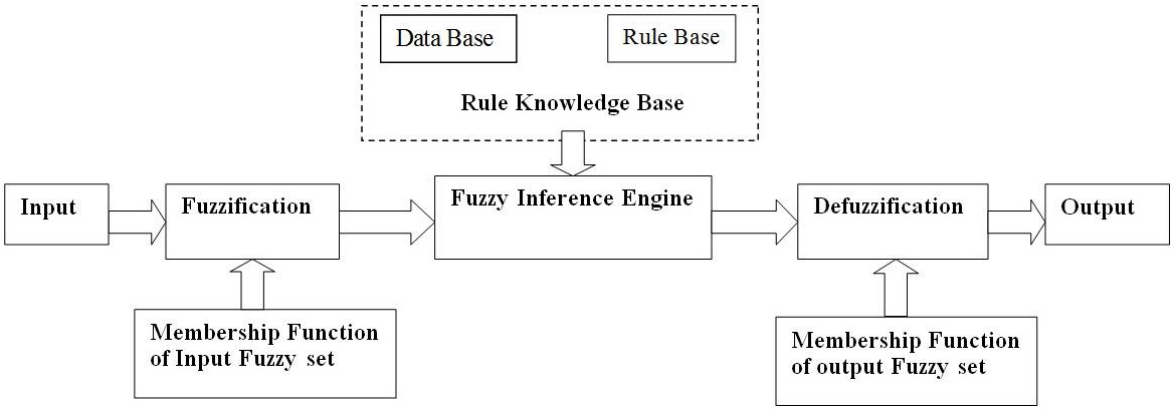

Figure 3. Fuzzy logic mechanism.

In present investigation, "grey relation fuzzy grade" is calculated in a view to optimize the considered input variables. The output "grey relation fuzzy grade" is ranged from 0 to 1. Optimization of the multiple correlated variables is performed by employing the concept of fuzzy logic. The output is aimed on achieving the highest value of GRFG. This work is carried out by considering the grey relation coefficient of MRR and TWR as input and GRFG as output in order to find out optimal condition. Fuzzy logic system is developed with the help of MATLAB 7.12.0.635 (Release 2011a). Figure 4 shows the block diagram of fuzzy model containing two variables (MRR and TWR) as input and GRFG as output.

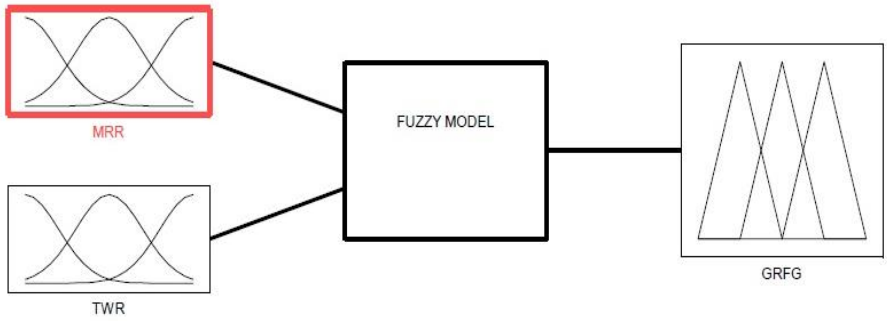

Figure 4. Block diagram of fuzzy model for GRFG.

The input parameters, i.e., grey relation coefficients of MRR and TWR are demonstrated by membership functions possessing five levels, very low (VL), low (L), medium (M), high (H) and very high (VH) as depicted in Figures 5 and 6. The output parameter (GRFG) is characterized by membership functions (*MF*) possessing seven levels, namely extremely low (EL), very low (VL), low (L), medium (M), high (H), very high (VH) and extremely high (EH) as depicted in Figure 7. The triangular membership function is chosen for both types of variables. The fuzzy rules form a group with two GRC (MRR and TWR), and single output of GRFG. Fuzzy rules (25 in number) are obtained on the basis of the fact that largest GRFG is best response. Table 6 shows the fuzzy rules in matrix form.

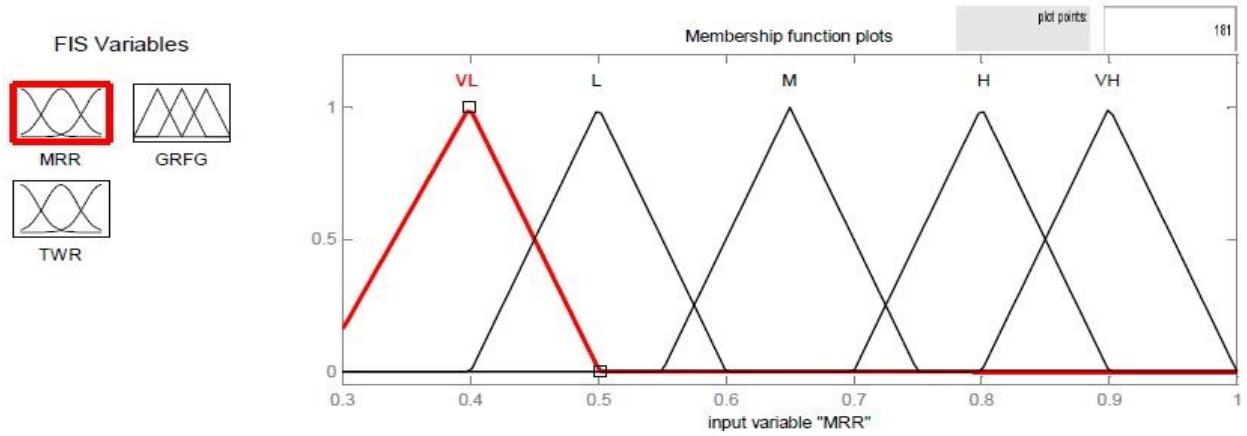

Figure 5. *MF* for MRR.

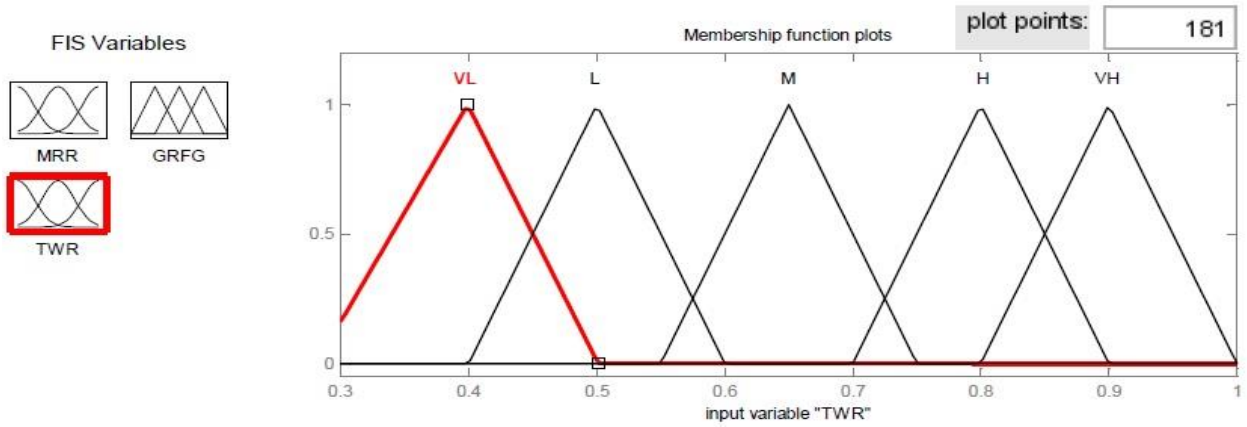

Figure 6. *MF* for TWR.

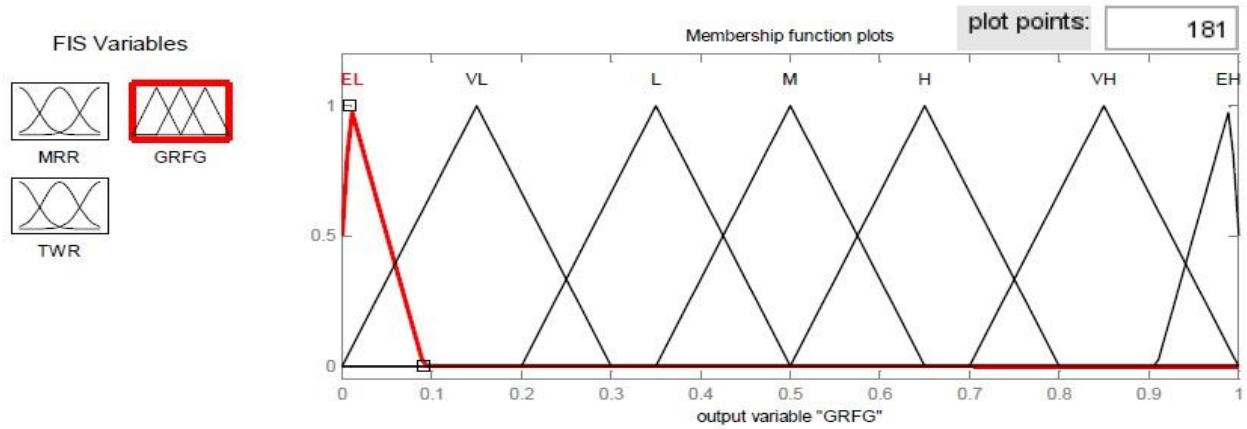

Figure 7. *MF* for GRFG.

Table 6. Fuzzy rules.

		GRC (MRR)				
		VS	S	M	L	VL
GRC (TWR)	VS	EL	VL	VL	L	M
	S	VL	L	L	M	S
	M	L	M	M	S	VS
	L	M	S	S	VS	VS
	VL	S	VS	VS	ES	ES

In addition, the input provided to fuzzy inference engine's rule editor is the grey relational coefficient of each response variable (MRR and TWR), as shown in Figure 8. Table 5 depicts the de-fuzzified values of each experimental run obtained through grey-fuzzy system. The response table for mean of the output parameter (GRFG) for each level of the input parameters is shown in Table 7. Figure 9 depicts the distribution of grey relational fuzzy grade for different experiments.

Table 7. Response table for GRFG.

Levels	Cobalt content	Work thickness	Profile of tool	Tool material	Grit size	Power rating
1.	0.7254	0.7122	0.6614	0.7227	0.6735	0.6099
2.	0.6607	0.6739	0.7248	0.7282	0.7760	0.7294
3.	-	-	-	0.6284	0.6298	0.7399
Max.–Min.	0.0647	0.0383	0.0634	0.0998	0.1462	0.13
Rank	4	6	5	3	1	2

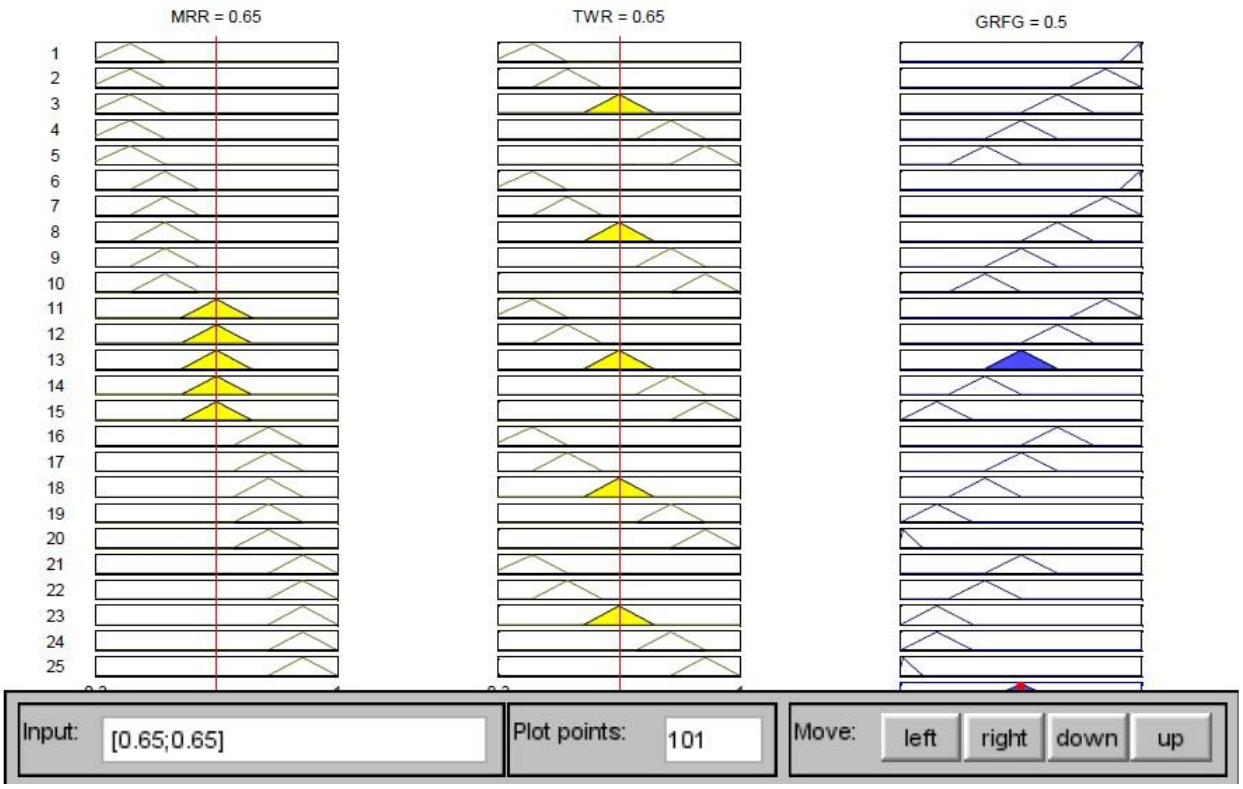

Figure 8. Rule viewer for GRFG.

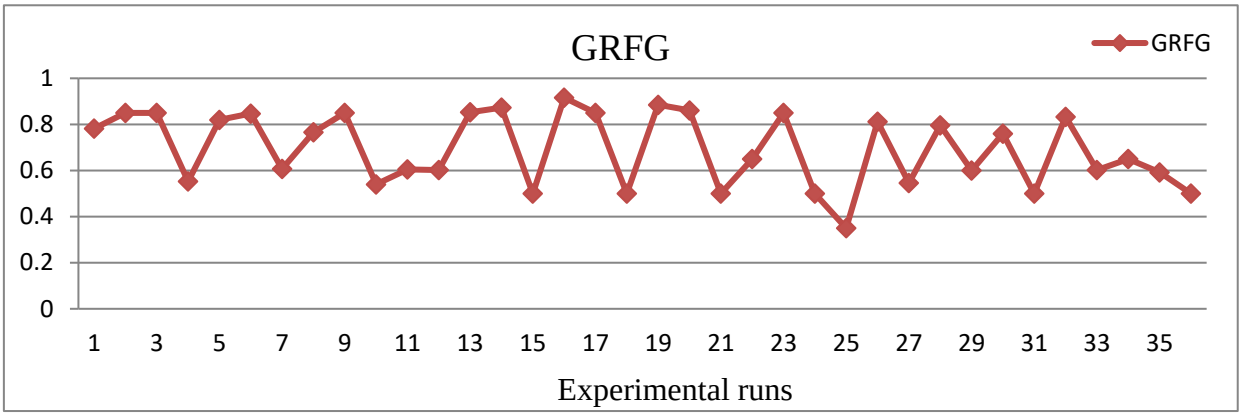

Figure 9. Distribution of grey relational fuzzy grade against experimental runs.

To determine the optimal combination, the highest grey relation fuzzy grade (GRFG) is to be located among all possible arrangements of the process parameters. Table 7 presents the average GRFG for each factor. The numeric terms in each column of factors are the highest GRFG for corresponding factor, which also indicates the best level for that factor. The difference between maximum and minimum value of GRFG at each levels represents the range for each factor. Highest range (max–min) of GRFG is given the first rank and the lower ranges are provided with lower ranks correspondingly. Control factor with larger range of GRFG possess more effect in ultrasonic machining of WC-Co composite. Abrasive grit size and power rating have strong effect on the machining characteristics, as observed from the GRFG analysis.

As shown in Figure 10, the optimal parametric setting is 6% cobalt in work material; work thickness: 3 mm; tool geometry: hollow; material of tool: silver steel; abrasive grit size: 320 (mesh) and power rating: 80%.

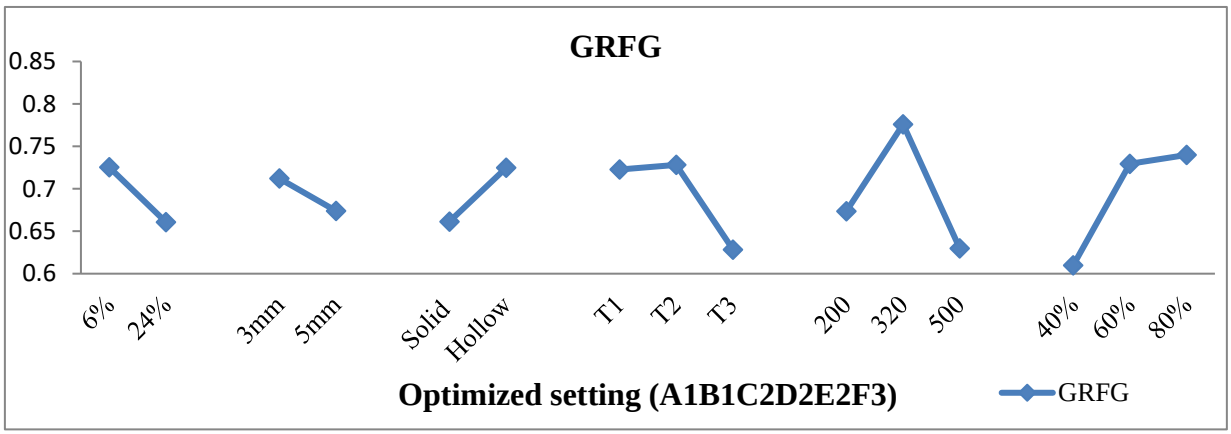

Figure 10. Mean effect plot for GRFG.

The ANOVA test has also been carried out for the GRFG and results are presented in Table 8. ANOVA results show that abrasive grit size has significant effect on the grey relation fuzzy grade.

Table 8. ANOVA results for GRFG.

Source	*DOF*	*F*	*P*
A	1	2.04	0.169
B	1	0.71	0.409
C	1	1.95	0.178
D	2	2.04	0.157
E	2	3.65	0.044*
F	2	3.38	0.054
A × D	2	0.40	0.674
B × D	2	1.11	0.349
C × D	2	0.24	0.793
Error	20		
Total	35		

A: cobalt content, B: thickness of work piece, C: tool profile, D: tool material, E: grit size, F: power rating.
* Significant at 95% confidence level.

The GRFG at optimized setting (A1B1C2D2E2F3) has been predicted using the following formula.

$$\mu_{GRFG} = \mu_{OA} + \sum_{k=1}^{n}(\mu_{GRFGo} - \mu_{OA}) \quad (6)$$

where, μ_{GRFGo} is the average value of GRFG for all experimental runs, μ_{OA} is the value of GRFG at optimal factor levels, n is the number of factors. Table 9 shows the predicted and experimental results. There is 20% improvement in the GRFG at optimized setting as compared with initial setting. At this optimized setting, the value of MRR and TWR are 0.0302 g/min and 0.0071 g/min, as compared to 0.0112 g/min and 0.0041 g/min at the initial setting.

Table 9. Predicted and confirmation experimental results at optimized setting.

	Initial setting	Optimized results	
		Predicted	Experimental
	A1B1C1D1E1F1	A1B1C2D2E2F3	A1B1C2D2E2F3
MRR	0.0112 g/min	0.0334 g/min	0.0302 g/min
TWR	0.0041 g/min	0.0057 g/min	0.0071 g/min
GRFG	0.782	0.941	-

5. Microstructure analysis

Selected machined samples were observed with scanning electron microscope (LEO, model-435VP) to investigate the surface characteristics. In ultrasonic machining, the surface characteristics are mainly affected by the effect of grit size, and power rating [29,30].

Figure 11 illustrates the microstructure of WC-Co composite after being machined with USM under the experimental conditions corresponding to experiment no. 15, at the magnification of 5000×. The parametric condition for this experimental run was consisting of fine sized abrasive grains and low level of power input. Hence, this corresponds to a condition of lower energy input

rate. In the SEM microstructure (Figure 11), there is no clear indication of the brittle fracture mode, due to the low energy input rate.

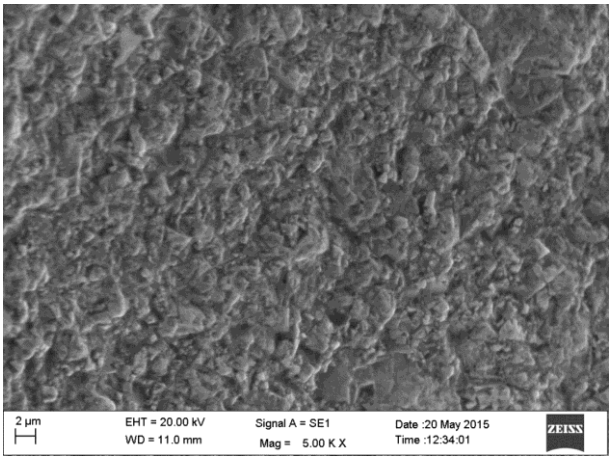

Figure 11. Microstructure for exp. no. 15.

Figure 12 exemplifies the microstructure of WC-Co composite after being machined with USM under the experimental conditions corresponding to experiment no. 23 at the magnification of 5000×. The parametric condition for this experimental run was consisting of medium sized abrasive grains and high level of power input. When highly energized (medium sized) abrasives make impact over the surface of work, few regions of pulled-off WC grains have been observed in the SEM image. A mixture of brittle and plastic deformation mode of work material removal has also been observed from the SEM image.

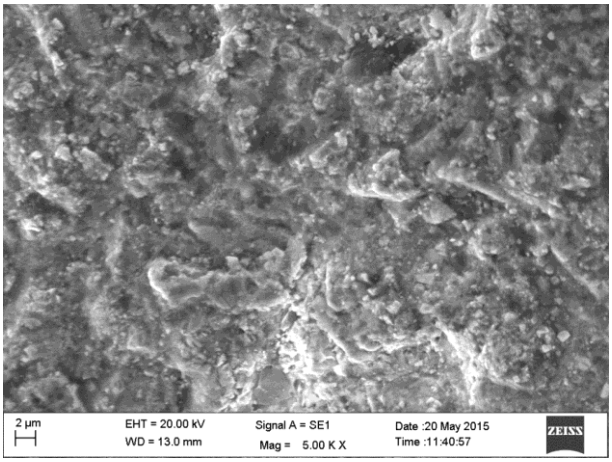

Figure 12. Microstructure for exp. no. 23.

Figure 13 shows the microstructure of WC-Co composite after processed with USM under the experimental conditions corresponding to experiment no. 36 at the magnification of 5000×. A huge amount of black pits is clearly visible from the microstructure due to the dislodgement of WC grains. Some regions have also been observed with the smeared out layers of cobalt binder material. In addition, a typical type of brittle fracture has been found for this particular experimental run.

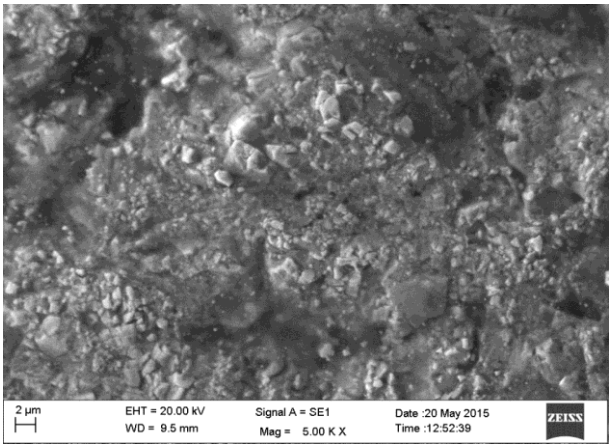

Figure 13. Microstructure for exp. no. 36.

Figure 14 shows the edge of the drilled hole at 200×. Moreover, there is no evidence of any micro-cracking. Figure 15 shows the machined sample with holes drilled under different experimental runs. The drilled holes have a straight cylindrical profile and the exit side has little appearance of chipping due to non uniform wear of the tool face.

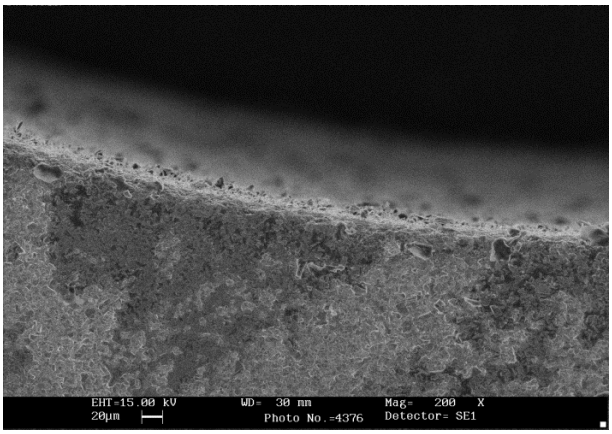

Figure 14. Shows the edge quality.

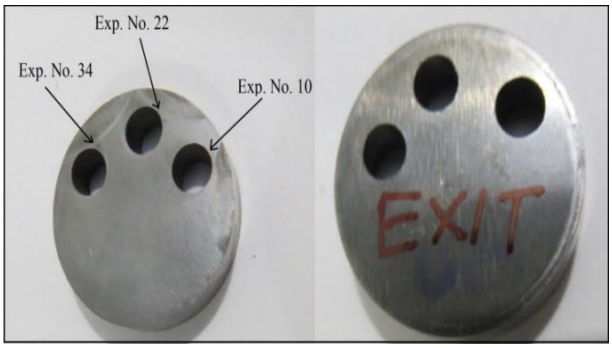

Figure 15. Entrance and exit sides of drilled holes.

6. Conclusions

The current research work has been focused at the application of grey relational analysis based fuzzy logic for the purpose of optimization of multiple performance characteristics in ultrasonic machining of WC-Co composite. Following conclusions could be drawn from this work:

- Abrasive grit size and power rating have been observed as most significant parameters for GRFG. The optimized setting is cobalt content: 6%; work thickness: 3 mm; tool geometry: hollow; material of tool: silver steel; abrasive grit size: 320 (mesh) and power rating: 80%.
- At optimized setting, an improvement of 20% in the GRFG has been observed at the optimized setting, as compared to initial setting. At this optimized setting, the values of MRR and TWR are 0.0302 g/min and 0.0071 g/min.
- The mode of material deformation has been observed from microstructure analysis and the parameters, i.e., work material properties, grit size, and power rating were revealed as the most crucial for on which deformation mode depends. The brittle fracture has been observed as a major mode of material deformation.
- No micro cracking has been observed at the edge of the drilled hole, although minor chipping has been observed at the exit face.

Conflict of interest

The authors declare that there is no conflict of interest regarding the publication of this paper.

References

1. Singh RP, Kumar J, Kataria R, et al. (2015) Investigation of the machinability of commercially pure titanium in ultrasonic machining using graph theory and matrix method. *J Eng Res* 3: 75–94.
2. Kataria R, Kumar J, Pabla BS (2015) Experimental Investigation and Optimization of Machining Characteristics in Ultrasonic Machining of WC-Co Composite using GRA Method. *Mater Manuf Process* 31: 685–693.
3. Lalchhuanvela H, Doloi B, Battacharyya B (2012) Enabling and Understanding Ultrasonic Machining of Engineering Ceramics Using Parametric Analysis. *Mater Manuf Process* 27: 443–448.
4. Komaraiah M, Reddy PN (1993) A study on the influence of workpiece properties in ultrasonic machining. *Int J Mach Tool Manu* 33: 495–505.
5. Kumar J, Khamba JS (2009) An investigation into the effect of work material properties, tool geometry and abrasive properties on performance indices of ultrasonic machining. *Int J Mach Mach Mater* 5: 347–366.
6. Dam H, Schreiber MP, Quist P (1995) Productivity, surface quality and tolerances in ultrasonic machining of ceramics. *J Mater Process Tech* 51: 358–368.
7. Kataria R, Kumar J, Pabla BS (2015) Experimental Investigation into the Hole Quality in Ultrasonic Machining of WC-Co Composite. *Mater Manuf Process* 30: 921–933.
8. Kataria R, Kumar J (2015) Machining of WC-Co composites—A review. *Mater Sci Forum* 808: 51–64.

9. Abdullah A, Shabgard MR, Ivanov A, et al. (2009) Effect of ultrasonic-assisted EDM on surface integrity of cemented tungsten carbide (WC-Co). *Int J Adv Manuf Tech* 41: 268–280.
10. Bhavsar SN, Aravindan S, Rao V (2012) Machinability study of cemented carbide using focused ion beam (FIB) milling. *Mater Manuf Process* 27: 1029–1034.
11. Gadalla AM, Tsai W (1989) Machining of WC-Co composites. *Mater Manuf Process* 4: 411–423.
12. Jahan M, Wong YS, Rahman M (2012) Experimental investigation into the influence of major operating parameters during micro-electro discharge drilling of cemented carbide. *Mach Sci Technol* 16: 131–156.
13. Kung KY, Horng JT, Chiang KT (2009) Material removal rate and electrode wear ratio study on the powder mixed electrical discharge machining of cobalt-bonded tungsten carbide. *Int J Adv Manuf Tech* 40: 95–104.
14. Mahdavinejad RA, Mahdavinejad A (2005) ED machining of WC-Co. *J Mater Process Tech* 162–163: 637–643.
15. Yadav SKS, Yadav V (2013) Experimental investigation to study electrical discharge diamond cutoff grinding (EDDCG) machinability of cemented carbide. *Mater Manuf Process* 28: 1077–1081.
16. Ramulu M (2005) Ultrasonic machining effects on the surface finish and strength of silicon carbide ceramics. *Int J Manuf Tech Manage* 7: 107–125.
17. Kumar V, Khamba JS (2010) An investigation into the ultrasonic machining of co-based super alloy using the taguchi approach. *Int J Mach Mach Mater* 7: 230–243.
18. Kumar J, Khamba JS, Mohapatra SK (2009) Investigating and modelling tool-wear rate in the ultrasonic machining of titanium. *Int J Adv Manuf Tech* 41: 1107–1117.
19. Hocheng H, Kuo KL, Lin JT (1999) Machinability of zirconia ceramic in ultrasonic drilling. *Mater Manuf Process* 14: 713–724.
20. Singh R, Khamba JS (2008) Comparison of slurry effect on machining characteristics of titanium in ultrasonic drilling. *J Mater Process Tech* 197: 200–205.
21. Majeed MA, Vijayaraghvan L, Malhotra SK, et al. (2008) Ultrasonic machining of Al_2O_3/$LaPO_4$ composites. *Int J Mach Tool Manu* 48: 40–46.
22. Kumar J, Khamba JS, Mohapatra SK (2008) An investigation into the machining characteristics of titanium using ultrasonic machining. *Int J Mach Mach Mater* 3: 143–161.
23. Dvivedi A, Kumar P (2007) Surface quality evaluation in ultrasonic drilling through the Taguchi technique. *Int J Adv Manuf Tech* 34: 131–140.
24. Komaraiah M, Manan MA, Reddy PN, et al. (1988) Investigation of surface roughness and accuracy in ultrasonic machining. *Precis Eng* 10: 59–68.
25. Kumar J, Khamba JS (2008) An Experimental study on ultrasonic machining of pure titanium using designed experiments. *J Braz Soc Mech Sci* 30: 231–238.
26. Ross PJ (1996) *Taguchi Techniques for Quality Engineering: loss function, orthogonal experiments, parameter and tolerance design*, New York: McGraw Hill.
27. Pan LK, Wang CC, Wei SL, et al. (2007) Optimizing multiple quality characteristics via Taguchi method-based Grey analysis. *J Mater Process Tech* 182: 107–116.
28. Kataria R, Kumar J (2014) A Comparison of the different Multiple response optimization techniques for turning operation of AISI O1 tool steel. *J Eng Res* 2: 161–184.

29. Kumar J (2014) Investigation into the surface quality and micro-hardness in the ultrasonic machining of titanium (ASTM GRADE-1). *J Braz Soc Mech Sci* 36: 807–823.
30. Kataria R, Kumar J, Pabla BS (2016) Experimental investigation of surface quality in ultrasonic machining of WC-Co composites through Taguchi method. *AIMS Mater Sci* 3: 1222–1235.

AIMS Press